

Formations of OH($X^2\Pi$, $A^2\Sigma^+$) in the Reaction of NH($^3\Sigma^-$) with NO in Incident Shock Waves

Keiichi YOKOYAMA, Yasuo SAKANE, and Takayuki FUENO*

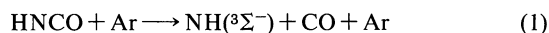
Department of Chemistry, Faculty of Engineering Science, Osaka University, Toyonaka, Osaka 560
(Received January 28, 1991)

Gaseous mixtures of HNCO and NO diluted in Ar were heated by incident shock waves to about 3500 K to investigate the bimolecular reaction of NH($^3\Sigma^-$) with NO. Ultraviolet emissions from the excited NH($A^3\Pi$) and OH($A^2\Sigma^+$) were monitored to determine the rate constants for the ground-state reaction NH($^3\Sigma^-$) + NO \rightarrow N₂ + OH($X^2\Pi$). The branching ratio defined as the rate constant for the formation of OH relative to that for the NH($^3\Sigma^-$) decay was found to be 0.32 ± 0.07 at the shock-wave temperature adopted. An intense spike of chemiluminescence due to OH($A^2\Sigma^+ \rightarrow X^2\Pi$) was observed, a finding which indicates a possible participation of the channel NH($^3\Sigma^-$) + NO \rightarrow N₂ + OH($A^2\Sigma^+$) at high temperatures.

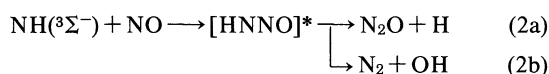
We have previously studied the reaction of NH($^1\Delta$) with NO in the gas phase at room temperature.¹⁾ The results have been in essence (1) that the reaction should proceed through an intermediacy of an adduct radical HNNO and (2) that the subsequent decomposition of HNNO gives rise to N₂O + H in prevalence over the channel leading to N₂ + OH. Ab initio configuration-interaction (CI) calculations of the potential energy profiles¹⁾ rationalized the experimental results.

Gas-phase reaction of NH($^3\Sigma^-$) with NO is intriguing in connection with the above-mentioned chemistry of NH($^1\Delta$) on one hand and with the issue of the process control for fuel combustions on the other. The reaction has already received interest by several groups of workers,^{2–7)} who unanimously claim that NH($^3\Sigma^-$) decays essentially at the collision-controlled rate, the rate constant being on the order of 10^{13} cm³ mol⁻¹ s⁻¹. However, product identification as the most important phase of chemical kinetics has remained unsettled.

In the present study, we intend to elucidate the kinetic feature of the NH($^3\Sigma^-$)–NO system, paying due attention to the time-dependent behavior of products. For this purpose, we have shock-heated the HNCO/NO/Ar mixtures of varying composition to ca. 3500 K, to let the NH($^3\Sigma^-$) entity generated by the thermal decomposition⁸⁾



react with the coexisting NO. In analogy to the case of NH($^1\Delta$), the reaction is expected to proceed in the following manner:



Unfortunately, however, N₂O if formed by reaction (2a) is liable to be readily decomposed into N₂ + O under the experimental conditions adopted. Thus, monitoring the OH radical to be formed by reaction (2b) will be a central issue of this study.

Experimental

The conventional incident shock tube described in a pre-

vious study⁹⁾ was used. Only the optical arrangement was altered. Time-resolved emission spectra were observed in the spectral region of 337.0 ± 3.0 nm for NH($A^3\Pi$ – $X^3\Sigma^-$) and 309.1 ± 3.0 nm for OH($A^2\Sigma^+$ – $X^2\Pi$). A Nikon-P250 grating monochromator with 1200 lines/mm and $F=4.5$ and a Hamamatsu 1P28 photomultiplier were used without lens or concave mirror. Time resolution arising from the observation volume was about 2 μ s. The signals were amplified with an electronic rise time $2.2RC$ less than 1 μ s and stored in a digital storage scope (Kawasaki Electronica KDS-103). Sample gases were shock-heated to about 3500 K in the pressure range of 210–870 Torr (1 Torr = 133.322 Pa). The compositions HNCO/NO/Ar of the samples used were 0.021/0.595/99.4 for the NH measurements and 0.048/1.10/98.9 and 0.053/0.616/99.3 for the OH measurements. The OH emission sensitivity was calibrated on the basis of the H₂/O₂/Ar experiments under the same conditions.

HNCO was synthesized by the reaction of potassium cyanate KCNO with excess stearic acid at 90–110 °C in a vacuum glass line. After removal of water using P₂O₅ and purification by means of trap-to-trap distillations at –80 °C, HNCO was stored at –196 °C and vaporized prior to use. NO (99.99%), H₂ (99.999%), O₂ (99.8%), N₂O (99.9%) (Takachiho Kagaku Inc.), and Ar (99.999%) (Seitetsu Kagaku Inc.) were used without further purification. Gas mixtures diluted in argon were stored in a 6-l Pyrex bulb for more than one day.

Results

(A) Decay of NH. The NH emission-time profiles recorded have exhibited a rapid rise within 10 to 20 μ s after the arrival of shock and subsequent decay during 40 to 100 μ s. From these decay curves we have evaluated the rate constants k_2 of the overall reaction (2), assuming a pseudo first-order decay law in excess of NO. The rate constant was determined to be $k_2 = (7.1 \pm 0.5) \times 10^{12}$ cm³ mol⁻¹ s⁻¹ at ca. 3500 K.

Figure 1 shows the Arrhenius plots of the reported experimental k_2 values at various temperatures including the value obtained in the present study. A negative temperature dependence is evident. The plotted points are best fitted by the Arrhenius equation, $k_2 = A \exp(-E_a/RT)$, with $A = (7.8 \pm 0.6) \times 10^{12}$ cm³ mol⁻¹ s⁻¹ and $E_a = -(3.5 \pm 0.3)$ kJ mol⁻¹. The results indicate that the association step (HNNO formation) involving no

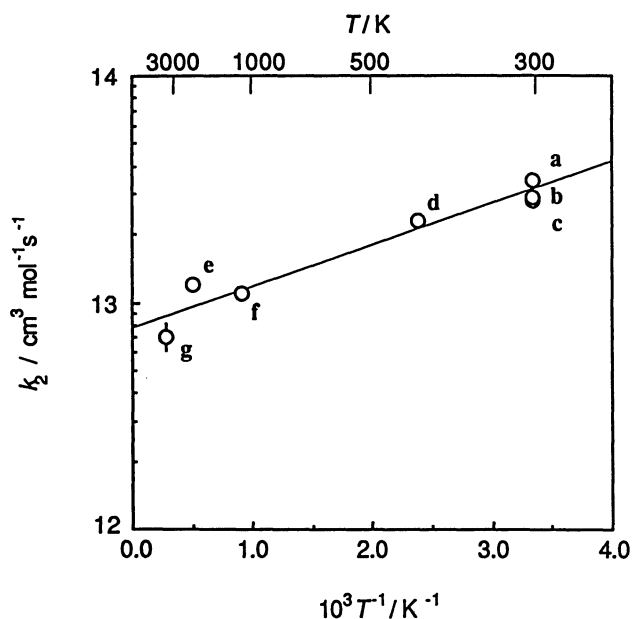


Fig. 1. Arrhenius plots of k_2 . a, Harrison et al.²⁾; b, Hansen et al.³⁾; c, Cox et al.⁵⁾; d, Gordon et al.⁴⁾; e, Dean et al.⁶⁾; f, Kondo⁷⁾; g, the present work.

potential energy barrier should be rate-controlling.

(B) Formation of OH. In the OH emission-time profiles, an intense emission was observed during a period of initial 30 μs , as is shown in Fig. 2. We attribute this emission to the $\text{OH}(\text{A}^2\Sigma^+ \rightarrow \text{X}^2\Pi)$ chemiluminescence, as will be discussed later. After the intense spike, almost steady or slowly increasing emission profiles were observed. These latter emissions are due to $\text{OH}(\text{A}^2\Sigma^+)$ which is in thermal equilibration with $\text{OH}(\text{X}^2\Pi)$. Thus, the emission intensity of this steady part directly corresponds to the concentration of $\text{OH}(\text{X}^2\Pi)$.

In order to determine the rate constant k_{2b} and hence the branching ratio $\beta \equiv k_{2b}/k_2$, we have decided to recourse to the computer simulation technique. Thus, we intend to search for the value of k_{2b} that will best reproduce the time-concentration profiles of OH observed under the varying experimental condition. To this end, we have invoked several elementary reactions to be considered concurrently at high temperatures. The elementary steps chosen for the simulation are listed in Table 1, together with pertinent Arrhenius parameters. For reaction (1), we have chosen the most recent kinetic data obtained by Hanson et al.⁹⁾ For

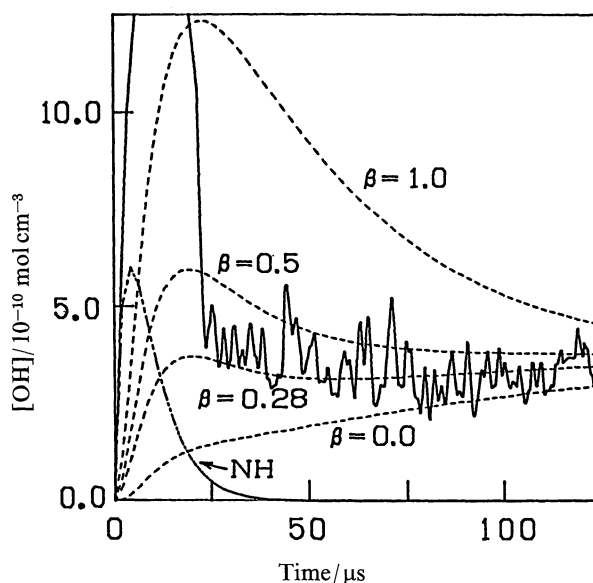


Fig. 2. Comparisons of the computed OH concentration profiles (---) with the observed (—). $T_2 = 3637\text{ K}$, $P_2 = 846\text{ Torr}$, $\text{HNCO}/\text{NO}/\text{Ar} = 0.053/0.613/99.33$.

Table 1. Elementary Reactions Used for the Simulations of the Time-Concentration Profiles of the OH Radical

No.	Reaction ^{a)}	$\log A$	n	E_a	Ref.
		$\text{cm}^3 \text{mol}^{-1} \text{s}^{-1}$		kJ mol^{-1}	
1	$\text{HNCO} + \text{Ar} \rightarrow \text{NH} + \text{CO} + \text{Ar}$	35.51	-5.11	460	9
2a	$\text{NH} + \text{NO} \rightarrow \text{N}_2\text{O} + \text{H}$	$(1-\beta)k_2$	0	0	This study
2b	$\rightarrow \text{OH} + \text{N}_2$	βk_2	0	0	This study
3	$\text{NH} + \text{NH} \rightarrow \text{N}_2 + 2\text{H}$	13.65	0	0	8
4	$\text{NH} + \text{Ar} \rightarrow \text{N} + \text{H} + \text{Ar}$	14.42	0	316	8
5	$\text{H} + \text{HNCO} \rightarrow \text{NH}_2 + \text{CO}$	14.04	0	223	8
6	$\text{NH}_2 + \text{Ar} \rightarrow \text{NH} + \text{H} + \text{Ar}$	23.50	-2.0	382	9
7	$\text{NH} + \text{CO} \rightarrow \text{CN} + \text{OH}$	13.00	0	0	10
8	$\text{OH} + \text{H} \rightarrow \text{H}_2 + \text{O}$	9.90	1	29	11
		10.26 ^{b)}	1 ^{b)}	37 ^{b)}	11
9	$\text{OH} + \text{O} \rightarrow \text{O}_2 + \text{H}$	13.40	0	0	11
		14.34 ^{b)}	0 ^{b)}	70.3 ^{b)}	11
10	$\text{OH} + \text{H}_2 \rightarrow \text{H}_2\text{O} + \text{H}$	13.34	0	21.7	11
11	$\text{OH} + \text{Ar} \rightarrow \text{O} + \text{H} + \text{Ar}$	18.90	-1	439	11
12	$\text{NO} + \text{H} \rightarrow \text{OH} + \text{N}$	12.40	0.5	201	11
13	$\text{N}_2\text{O} + \text{Ar} \rightarrow \text{N}_2 + \text{O} + \text{Ar}$	14.70	0	243	11

a) The rate constant $k = AT^n \exp(-E_a/RT)$ $\text{cm}^3 \text{mol}^{-1} \text{s}^{-1}$. b) For the reverse processes.

reactions (2a) and (2b) of our present interest, we use the rate constants $(1-\beta)k_2$ and βk_2 respectively, where k_2 is the above-mentioned rate constant for the net decay of NH. Reactions 3 through 6 are those elementary processes which are known to be important in simulating the time-concentration profile of $\text{NH}(\text{}^3\Sigma^-)$ after its generation by reaction (1).⁸⁾ The remaining reactions are all those that are related somehow with the OH radical. Reaction (7) in particular is the key reaction which has turned up to be of importance in the high temperature region above 2300 K.¹⁰⁾ The rate constants for reactions (8) through (13) were all taken from the literature.¹¹⁾

An example of the curve-fittings by simulation is shown in Fig. 2. As can be seen in Fig. 2, the calculated OH concentration first tends to increase with the decaying NH concentration. The OH concentration observed in this sample run stays at a nearly constant level of $3 \times 10^{-10} \text{ mol cm}^{-3}$ over the time period of 25–125 μs . The curve simulated under the assumption that $\beta=1.0$ definitely overestimates the OH concentration. It appears that the best fit of the calculated curve to the observed is attainable when β is assigned a value of 0.28. Note that the OH concentration approaches the experimentally observed steady level even when reaction (2b) has been assumed to make no contribution at all, i.e., $\beta=0$. This is simply because of the situation that reactions (7) and (12) can make significant contributions in the prolonged time region considered.

Computer simulations as delineated above have been conducted for a total of 9 runs. Results for typical runs are summarized in Table 2, together with the relevant experimental data. The values of β appear to be nearly constant at 0.32 ± 0.07 on the average, the allowance limit attached being the probable error. Taking this branching ratio as granted, the branching ratio for reaction (2a) is estimated to be 0.68 ± 0.07 which is in good agreement with the ratio 0.7 deduced previously for the case of the reaction of $\text{NH}(\text{}^1\Delta)$ at room temperature.¹⁾

Discussion

(A) Branching Ratio. The branching ratio depends on the excess energy and temperature. We have calculated the branching ratios at 300 K and 3500 K on the basis of the RRKM theory. Since the reactions to be

taken into account are only (2a) and (2b), calculations of only the ratio k_{2a}/k_{2b} suffice.

According to the basic RRKM theory, the ratio of the specific rate constants is given by

$$\frac{k_{2a}(E)}{k_{2b}(E)} = \frac{N_a(E-E_a)}{N_b(E-E_b)} \quad (\text{I})$$

Here, $k_{2i}(E)$, i being a or b, is the rate constant at a specific energy E , which is measured from the potential energy minimum for HNNO; E_i is the barrier height for reaction (2*i*); and $N_i(E-E_i)$ is the number of available states for the respective transition states with an energy in excess over E_i . In order to obtain the ratio k_{2a}/k_{2b} Eq. I need be integrated over the energy distribution. We assume that chemically activated HNNO upon its formation by the association of NH with NO would undergo fragmentation before collisional stabilization affects the internal energy distribution. Thus, we may write approximately¹²⁾

$$\frac{k_{2a}}{k_{2b}} = \int_{E_0}^{\infty} \left(\frac{N_a(E-E_a)}{N_b(E-E_b)} \right) F(E) dE \quad (\text{II})$$

where E_0 is the reactant potential energy level and where $F(E)$ is the energy distribution function:

$$F(E) = \frac{N(E-E_0) \exp(-E/kT)}{\int_{E_0}^{\infty} N(E-E_0) \exp(-E/kT) dE} \quad (\text{III})$$

with $N(E-E_0)$ as the number of available states for HNNO having energy in excess over E_0 .

In calculating the ratio k_{2a}/k_{2b} by Eq. II, the energy humps, E_0 , E_a and E_b were all taken from the results of our previous CI calculations (Fig. 3).¹⁾ With the vibration zero-point energy corrections, they are 234, 180, and 197 kJ mol^{-1} , respectively. The values of N , N_a , and N_b were all evaluated by the Whitten–Rabinovitch approximation,¹³⁾ using the fundamental vibrational frequencies obtained from the ab initio SCF calculations. At 3500 K, k_{2a}/k_{2b} has come out to be 3.2. It follows that $\beta=0.24$, in reasonable agreement with the experimental value of 0.32. The small discrepancy between the calculated and observed values may be due to the uncertainty attached to the calculated potential energies of the transition states as well as the dynamically preferential formation of $\text{OH}(\text{}^2\Pi) + \text{N}_2$, i.e. the non-statistical behavior of HNNO. Either way, it is confirmed that a sizable amount of OH can arise from reaction (2), although it may not innately be the main product.

Table 2. Run Conditions and the Branching Ratio β for the Reaction $\text{NH}(\text{}^3\Sigma^-) + \text{NO} \rightarrow \text{N}_2 + \text{OH}$

No.	[Ar]	[HNCO] ₀	[NO] ₀	<i>P</i> ₂	<i>T</i> ₂	ρ_{21}	β
	$10^{-6} \text{ mol cm}^{-3}$	$10^{-9} \text{ mol cm}^{-3}$		Torr	K		
1	1.26	0.61	13.9	279	3539	3.69	0.29
2	1.12	0.59	6.9	233	3355	3.67	0.25
3	1.79	0.95	11.0	380	3404	3.68	0.29
4	1.80	0.95	11.1	359	3207	3.66	0.38
5	3.73	1.98	23.0	846	3637	3.70	0.28
6	4.05	2.15	25.0	871	3444	3.68	0.44

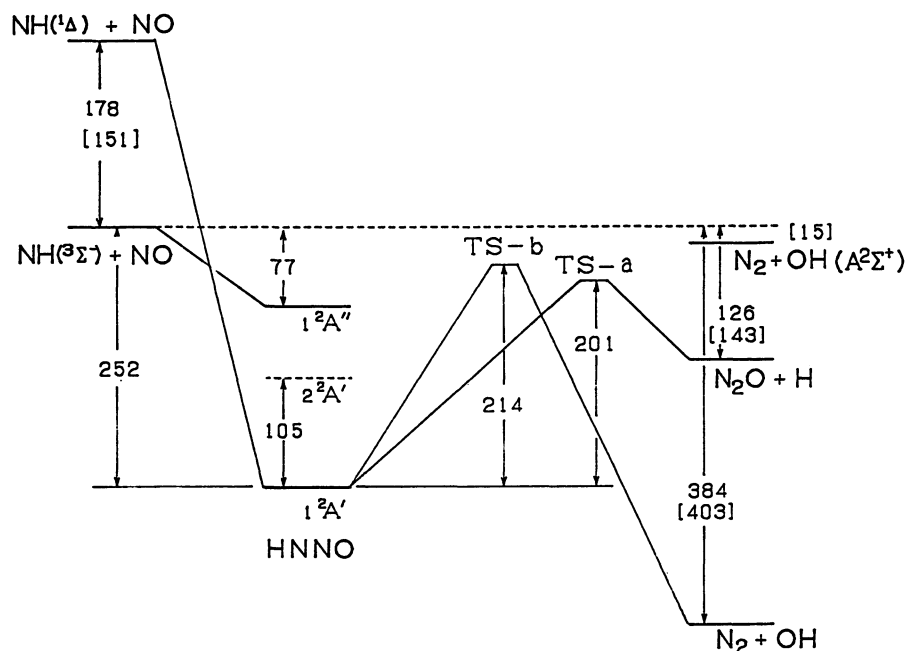


Fig. 3. Potential energy profiles calculated by the MRD-CI(4-31G**//4-31G**) procedure.¹⁾ The energy gaps shown are in units of kJ mol^{-1} . The values given in brackets are those obtained from the relevant thermochemical data.¹⁶⁾ TS-a and TS-b denote the transition states located for the unimolecular steps of reactions (2a) and (2b), respectively.

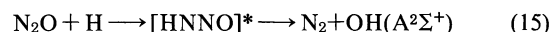
Further, we have obtained $\beta=0.31$ and 0.19 for $\text{NH}(^1\Delta)+\text{NO}$ and $\text{NH}(\Sigma^-)+\text{NO}$, respectively, both at 300 K . The former value is in good accord with our previous results of the N_2O quantum yield measurements [$\phi_{\text{N}_2\text{O}}=1-\beta=0.7$].¹⁾

Incidentally, the above discussions presume that the HNNO adduct to be formed from $\text{NH}(\Sigma^-)+\text{NO}$ be in its ground electronic state (X^2A'), just as in the case of the $\text{NH}(^1\Delta)+\text{NO}$ system. The presumption will be acceptable in view of the possibility of an effective "conical" crossing between the two doublet surfaces of the interacting $\text{HN}\cdots\text{NO}$ system.

(B) OH Chemiluminescence. The initial spike in the OH emission profiles is attributed to the $\text{OH}(A^2\Sigma^+ \rightarrow X^2\Pi)$ chemiluminescence on the basis of the following observations. First, the emission was observed in the absorption experiments as well. That is, in order to monitor the OH concentration, we applied also the absorption technique using a $\text{He-H}_2\text{O}$ microwave-discharge lamp as a light source of the OH absorption. Obtained profiles were of course quite different from the emission profiles, but the initial spike was still an intense emission in contrast to the pattern of the subsequent steady part due to absorption. Second, we confirmed that the peak height of the spike attained a maximum at the wavelength 308 nm , which was consistent with the $\text{OH}(A-X)$ emission band. Third, when temperature was raised from 3500 K to 4100 K , the peak height did not increase correspondingly as did the subsequent steady part. Fourth, when $\text{N}_2\text{O}/\text{H}_2/\text{Ar}$ gas mixtures

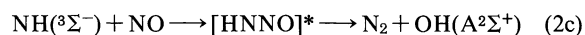
were shock-heated, a similar intense spike was observed. In this connection, when O_2 or H_2O , instead of NO , was added to the HNCO/Ar gas mixtures, no emission spike was observed.

A few words will be in order regarding the initial spike which was observed in the reaction system $\text{N}_2\text{O}+\text{H}_2$. The OH chemiluminescence will be possible in the manner as follows:



It should be noted that the initial step of reaction (15) is nothing but the reverse process of the unimolecular step of reaction (2a).

The formation of $\text{OH}(A^2\Sigma^+)$ is formally represented as



The branching ratio of reaction (2c) has been estimated from the comparison of the chemiluminescence intensity with the thermal emission intensity. We assume that the relative intensity is equal to the rate of the $\text{OH}(A^2\Sigma^+)$ formation through reaction (2c) relative to that through the excitation of $\text{OH}(X^2\Pi)$ on collisions with Ar:

$$\frac{I_{\text{chem}}}{I_{\text{therm}}} = \frac{k_{2c}[\text{NH}(\Sigma^-)][\text{NO}]}{k_{ex}[\text{OH}(X^2\Pi)][\text{Ar}]} \quad (IV)$$

Here, k_{ex} denotes the rate constant for the collisional

excitation, which may be assumed to be to $k_{\text{quench}}K_{\text{ex}}$, where k_{quench} is the quenching rate constant¹⁴⁾ and where K_{ex} is the equilibrium constant between $\text{OH}(X^2\Pi)$ and $\text{OH}(A^2\Sigma^+)$. As a result, we have estimated $k_{2c} \leq 7 \times 10^{10} \text{ cm}^3 \text{ mol}^{-1} \text{ s}^{-1}$. The branching ratio for reaction (2c) is thus less than 0.01. Considering that reaction (2c) is only slightly exothermic, the reaction is expected to have a significantly high barrier.

Hoffmann et al. have already reported on the same chemiluminescence arising from the reaction of N_2O with the H atom having a kinetic energy of ca. 2.5 eV under bulk conditions (single-collision and arrested-relaxation).¹⁵⁾ At lower H-atom kinetic energies (ca. 1.8 eV), however, there was no chemiluminescence. Since the $\text{N}_2\text{O} + \text{H}$ system lies about 1.5 eV below the $\text{NH}(^3\Sigma^-) + \text{NO}$ system, the threshold energy for the production of $\text{OH}(A^2\Sigma^+) + \text{N}_2$ from $\text{NH}(^3\Sigma^-) + \text{NO}$ should lie 0.3 to 1.0 eV above the energy level for $\text{NH}(^3\Sigma^-) + \text{NO}$.

Previous ab initio MO calculations¹⁾ have revealed that the ground state $\text{HNNO}(1^2A')$ surface is correlated to $\text{OH}(X^2\Pi) + \text{N}_2$ adiabatically. Therefore, it is most likely that for the first excited state $\text{HNNO}(2^2A')$ an adiabatic potential energy surface correlates to $\text{OH}(A^2\Sigma^+) + \text{N}_2$. The virtual excitation energy of the $\text{HNNO}(2^2A')$ at the equilibrium geometry of *cis*- $\text{HNNO}(1^2A')$ has been calculated by the MRD-CI method to be 105 kJ mol^{-1} , as is shown in Fig. 3. The excitation energy seems to be low enough for the internal conversion from $1^2A'$ to $2^2A'$ to take place thermally. For clear discussion of the dynamical mechanism of the formation of $\text{OH}(A^2\Sigma^+)$, MCSCF calculations on the excited state surface are required.

Conclusions

From the time-concentration profiles of the OH radicals formed in the shock-heated $\text{HNCO}/\text{NO}/\text{Ar}$ mixtures, the branching ratio of the reaction, $\text{NH}(^3\Sigma^-) + \text{NO} \rightarrow \text{N}_2 + \text{OH}(X^2\Pi)$, was determined to be 0.32 ± 0.07 . The experimental result was rationalized by the RRKM treatments of the product-determining step. A new

chemiluminescent reaction $\text{NH}(^3\Sigma^-) + \text{NO} \rightarrow \text{OH}(A^2\Sigma^+) + \text{N}_2$, was found, although it is a minor channel.

This work was supported by the Grant-in-Aid No. 61470007 from the Ministry of Education, Science and Culture.

References

- 1) T. Fueno, M. Fukuda, and K. Yokoyama, *Chem. Phys.*, **124**, 265 (1988).
- 2) J. A. Harrison, A. R. Whyte, and L. F. Phillips, *Chem. Phys. Lett.*, **129**, 346 (1985).
- 3) I. Hansen, K. Hoinghaus, C. Zetzsch, and F. Stuhl, *Chem. Phys. Lett.*, **42**, 370 (1976).
- 4) S. Gordon, W. Mulac, and P. Nangia, *J. Phys. Chem.*, **75**, 2087 (1971).
- 5) J. W. Cox, H. H. Nelson, and J. R. McDonald, *Chem. Phys.*, **96**, 175 (1985).
- 6) A. M. Dean, M. S. Chou, and D. Stern, *Int. J. Chem. Kinet.*, **16**, 633 (1984).
- 7) O. Kondo, Doctoral Dissertation, Osaka University (1982).
- 8) O. Kajimoto, O. Kondo, K. Okada, J. Fujikane, and T. Fueno, *Bull. Chem. Soc. Jpn.*, **58**, 3469 (1985).
- 9) J. D. Mertens, A. Y. Chang, R. K. Hanson, and C. T. Bowman, *Int. J. Chem. Kinet.*, **21**, 1049 (1989).
- 10) K. Yokoyama and T. Fueno, *Bull. Chem. Soc. Jpn.*, to be published.
- 11) F. Westley, "Table of Recommended Rate Constants for Chemical Reactions Occurring in Combustion," National Bureau of Standards, Washington, D. C. (1980).
- 12) W. N. Olmstead and J. I. Brauman, *J. Am. Chem. Soc.*, **99**, 4219 (1977).
- 13) G. Z. Whitten and B. S. Rabinovitch, *J. Chem. Phys.*, **38**, 2466 (1963).
- 14) K. H. Becker, D. Haaks, and Tatarczyk, *Chem. Phys. Lett.*, **25**, 564 (1974).
- 15) G. Hoffmann, D. Oh, and C. Wittig, *J. Chem. Soc., Faraday Trans. 2*, **85**, 1141 (1989).
- 16) M. W. Chase, Jr., C. A. Davies, J. R. Downey, Jr., D. J. Frurip, R. A. McDonald, and A. N. Syverud, "JANAF Thermochemical Tables," 3rd ed, National Bureau of Standards, Washington, D. C. (1985).